**ICMIEE20-027**

# A Numerical Study on Interaction of $A_0$-mode Lamb Wave with Cylindrical Hole in CFRP Composite Laminates

*M S Rabbi*[1,*], *K Teramoto*[2], *T I Khan*[2]
[1] Department of Mechanical Engineering, Chittagong University of Engineering & Technology, Chattogram-4349, BANGLADESH
[2] Department of Advanced Technology Fusion, Saga University, 1 Honjo-machi, Saga, 840-8502, JAPAN

**ABSTRACT**
This study represents the interaction of $A_0$-mode Lamb wave at a cylindrical hole in composite laminates focusing on its scattering characteristics. A 3-dimensional Finite Element Modeling (FEM) is used to discuss the effect of the stacking sequence in the wave propagation. An excitation signal of 30 kHz, modulated by Hanning window is allowed to propagate with plane strain condition in a defected squared shape laminate. Propagations of Lamb wave in 8-layered composite laminates with an identical defect are considered. It is found that the reflecting and transmitting characteristics of the incident wave dominated by the outermost layer and the pattern varied with different stacking sequences. The outcomes of this computational study help to the use of the $A_0$-mode Lamb wave for damage characterization and detection in composite laminates.

Keywords: Lamb wave, Cylindrical hole, CFRP, Directivity pattern.

## 1. Introduction

In recent years, Composite Laminates (CL) draws more attention in a wide spectrum of industries, especially in safety-critical applications such as aircraft primary structures, constructional structures, cars, rail vehicles, etc. Better strength & stiffness-to-weight ratios, controllability in fiber alignment, good acoustic and thermal insulation, low fatigue are the dominating advantages of CL. CL could be damaged during manufacturing as well as in long-term use in many ways and could be generated by fatigue, overload or impacts, which further leads to delamination, fiber breakage, voids, and matrix cracking. Lamb waves based health monitoring technique of infrastructure proved sensitive and efficient [1-2] from the last several decades as it increases the reliability and reduces the life-cycle cost for infrastructure. The perception regarding the scattering behavior of Lamb wave is an essential part in the application for detecting anomalies in structures. Number of researches has been carried out to investigate the Lamb wave interaction at various types of damage for isotropic material [3-5]. Due to the anisotropic nature of CL, researchers are yet to found the effective analytical solutions of Lamb waves scattering at defected region. Numerous investigations have been carried out through numerical simulation to understand the scattering of Lamb wave at through holes in the structure. Guo and Cawley studied the reflection of the $S_0$ mode Lamb wave in CL with plane strain assumption and it was shown that such type of mode is not useful to detect the delamination at the through-thickness locations [1]. The reflection behavior of fundamental mode Lamb waves from delamination of CL was studied by Hayashi and Kawashima [6]. It was found that $A_0$ mode Lamb wave is extensively responsive to the delamination type defect at all through-thickness locations.

In recent years, Lamb wave reflection and transmission characteristics in composites studied by CT Ng [7]. Hai et al. offered an analytical study of the $S_0$ Lamb mode reflection from a blind hole in a plate-like structure using the 3D theory [8]. They described the interaction of the high frequency Lamb waves with defects. Reza and Ng investigated guided wave (GW) based scattering behavior at delamination in composite beams and the mode conversion phenomena as well [9]. They conducted the 3D FE simulation and the result was verified by experimental studies. It was reported that, sizes and location of the flaw have crucial influence on the reflecting behavior of GW.

A NDE method using the $A_0$-mode to spot the position of the delamination along the thickness of a CL has been presented by Singh et al. by means of numerical and experimental studies [10]. Chiu et al. studied the reflection of the $A_0$-mode by delamination at the edge of a quasi-isotropic CL [11]. To interrogate the delamination, located at the mid-plane of the structure, they carried out the computational as well as the experimental studies. They concluded that the scattering behavior and amplitude remarkably influence by the ratio of flaw size to the wavelength. The interaction of $A_0$-mode Lamb waves with delamination using finite element simulations have been analyzed by Feng et al. [12]. Lamb waves propagation in a multiple layer laminate was compared with propagations obtained in a delaminated. Based on the comparison of the scattering characteristics between multi-layer laminate and single layer sub-laminate, they proposed a reference-free localization technique for damage identification.

* Corresponding author. Tel.: +88-01717300305
E-mail addresses: rabbi@cuet.ac.bd

This paper studies the $A_0$-mode Lamb wave scattering at a through-hole cylindrical flaw in CFRP laminate with different stacking sequence of unidirectional fiber directed layer. The exciting features of $A_0$-mode compared to its counterpart are (i) relatively easy to generate at low frequency, and (ii) shorter wavelength at the entire range of frequency. These leading characteristics of $A_0$-mode Lamb wave attracted considerable interest in quantitative damage evaluation [13-15].

This article is organized in the following way: Section 2 will discuss the fundamentals of CFRP laminate. Finite Element Modeling to generate the lamb wave will be explained in Section 3. Development of scattering directivity pattern of the scattered wave from the through-thickness hole in various composite laminates will be demonstrated in Section 4. Finally, concluding remarks will be stated in Section 5.

## 2. CFRP Laminate

CFRP represents Carbon Fiber Composite Laminate. The general constituents of the CFRP laminate are carbon strand and polymer. Among various matrixes, epoxy-resin is used as polymer in CFRP laminate. The fibers are usually 7-15 μm in width and has an overall thickness of the lamina is about 0.05-0.2 mm. Numerous laminae are stacked together in the equivalent or various ways to shape an overlay. The direction of the carbon fiber packed within the polymer has a greater influence in the degree of anisotropy in CFRP. According to the fiber orientation, unidirectional laminate, cross-ply laminate and angle-ply laminate are available. Fig. 1 depicted a typical example of CFRP laminate where the stacking sequence symmetrically balanced.

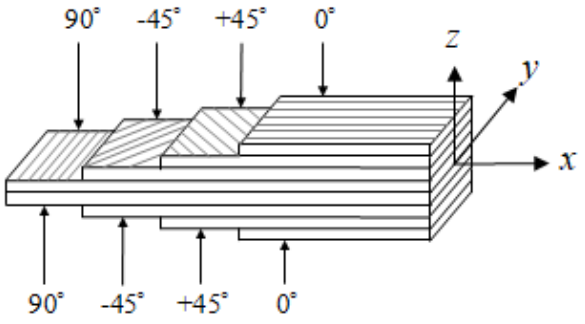


**Fig. 1** Typical stacking sequence of CL.

Fig. 1 illustrated that each of the unidirectional lamina, in together, formed a CFRP laminate. The $0^{\circ}$ lamina can be termed as horizontally transversely isotropic (HTI) material, the building block of composite laminated structures. Each of the lamina can be characterized by the generalized Hooke's law and follow the following formula:

$$[\sigma]=[C][\varepsilon] \tag{1}$$

In the aforementioned equation, the 4th order stiffness matrix [C] defines the properties of the material. The engineering constants of the HTI material is determined by micromechanical modelling [16] and given as $C_{11}$=96.0, $C_{22}$=9.60, $C_{12}$=3.60, $C_{23}$=7.01, $C_{55}$=3.30 (all values are in GPa). In this study, different stacking sequences (mentioned in Table 1) have been considered to observe the interaction of Lamb wave, focusing on the scattering directivity pattern where the incident wave interacted with a through hole.

**Table 1** CFRP laminate with various stacking sequence considered in this study (Numerical value i.e. 2, 4 denotes the number of repetitive lamina and 'S' stands for symmetric lamina).

| Composite laminate | Stacking sequence |
|---|---|
| Bi-directional | $[0/90]_{2S}$ |
| Bi-directional | $[0/90]_4$ |
| Bi-directional | $[+45/-45]_{2S}$ |
| Bi-directional | $[+45/-45]_4$ |
| Quasi-isotropic | $[0/+45/-45/90]_S$ |

To make the stacking, it is mandatory to find the stiffness matrix for different fiber orientation. This fiber orientation results in the directional dependence of the phase velocity. To investigate this criterion, it is mandatory to transform the 0º fiber orientation (HTI) to the required fiber orientation in a new coordinate system. A new stiffness matrix can be formulated by the following equation [17].

$$[C']=[T][C][T'] \tag{2}$$

Where [$C'$] denotes the stiffness matrix in the new coordinate system and [$T$] denotes the transformed matrix. These transformed components are directly involved to determine the characteristics of CFRP laminate. Based on these material characteristics, finite element modeling has been developed, discussed on the next section.

## 3. Numerical Modeling

A 3D FE computational analysis is conducted to study the interaction of Lamb wave in the CFRP laminate. Generation of the geometry and meshing are done in explicit type software LS-DYNA [18] and the simulations were done using the same platform. The laminates considered in this study consisting of the eight-ply unidirectional lamina with a various combination of 0º, +45º, -45º, and 90º fiber directed lamina. The specific mass of an individual lamina is considered 1500 kg/m$^3$ [19]. The length and width of the specimen is considered as 150 mm each having 1.6 mm of thickness where each lamina has a thickness of 0.2 mm. The wavelengths are calculated theoretically based on the material properties mentioned in Section 2 and found 7.36 mm in the 0º and 5.70 mm 90º direction. To ensure the number of nodes per wavelength for perfect prediction of wave propagation, a fine mesh

with dimension 0.5 mm × 0.5 mm (14 nodes) is used for the entire model [20]. The eight-node 3D reduced integration solid brick elements with hourglass control are considered to generate the flawless region of the 3D model whereas the surrounding of the cylindrical defect modelled using the combination of six-node wedge element. The time step is taken as 100 ns, which is sufficient to satisfy the conditions for the explicit type of finite difference numerical analysis [21]. The hourglass energy is found less than 2% of the internal energy for all carried out studies which sufficiently helpful to predict the Lamb wave field accurately.

At any particular location, the $A_0$-mode Lamb wave signal can be obtained by monitoring the normal ($z$) displacement of the elements located at the mid-section of the 3D model in the vertical direction. This guaranteed that only $A_0$-mode is detected as the $S_0$ and $SH_0$-mode have zero normal displacements at that location [21]. To find out the dispersion curve, a signal with a sample frequency has been excited from any specific point in a flawless $[0]_8$ laminate and gathered the velocity of the elements located 10 mm away from each other. The average velocity has been taken into account and the dispersion curve of $A_0$-mode Lamb wave is depicted in Fig. 2 [22]. It is found good agreement between the theoretical calculation (reported in Section 2) and the corresponding FE simulation.

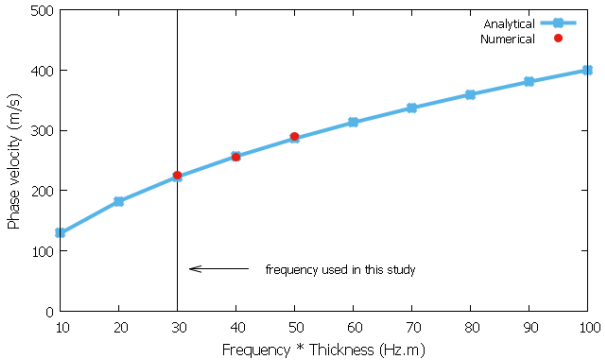


**Fig. 2** $A_0$-mode Lamb wave phase velocity dispersion curve for $[0]_8$ laminate (HTI material) of 1.0 mm in thickness.

Fig. 3 shows the decaying characteristics of the out-of-plane amplitude in the $[0]_8$ composite laminates as a function of distance from the excitation along the fiber direction. The values are normalized by the amplitude found at the distance of 10 mm.

To generate the cylindrical through-hole defect, elements are removed from the 3D model. To observe the reflection from the defect, a study is conducted in a $[0/90]_{2S}$ model with through-hole cylindrical defect, allowing the wave propagation from a half-circular transducer diameter of 0.9 mm 5-cycle Hanning windowed source (showed in Fig. 4) with a central frequency of 30 kHz and located at the middle of the left end. Contours of normal displacement of the particles taken into account and Fig. 5 shows the typical snapshots of the FE simulated normal displacement for a $[0/90]_{2S}$ laminate. After excitation from the left boundary of the model, wave incidents at the flaw boundary region, reflection and transmission immediately occurred throughout the entire defected area.

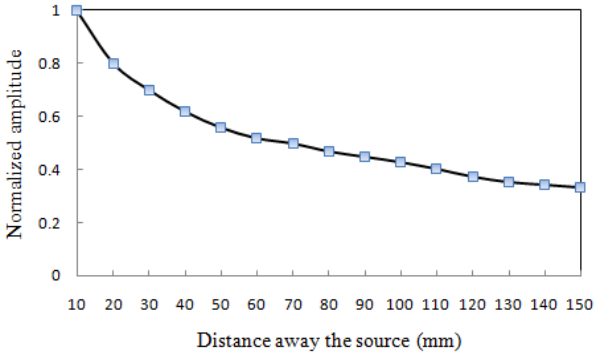


**Fig. 3** Normal amplitude as a function of wave propagation distance in the $[0]_8$ laminate (Normalized by its maximum value).

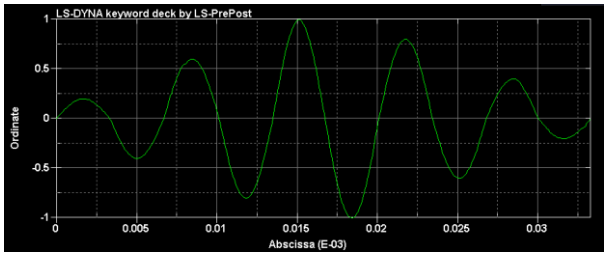


**Fig. 4** Input 5-cycle Hanning windowed excitation signal

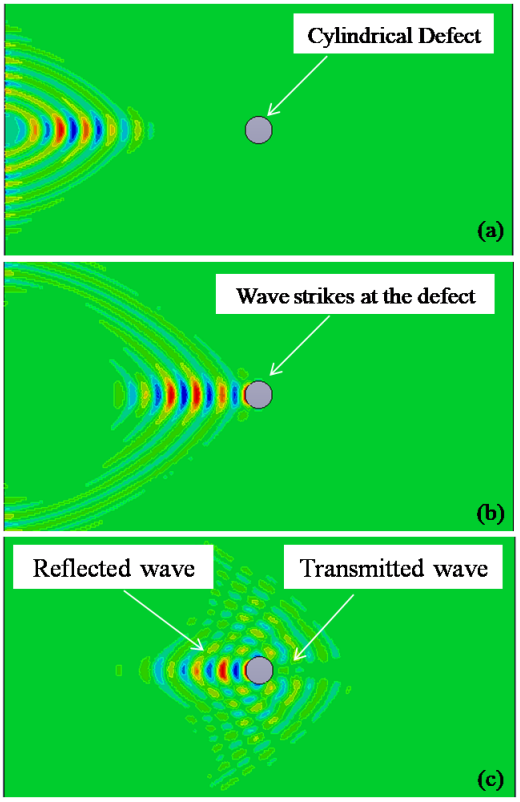


**Fig. 5** Photographs of the numerically simulated out-of-plane displacement for the $[0/90]_{2S}$ laminate (a) after the irradiation, (b) at the time of striking and (c) reflected and transmitted wave from the through-hole defect.

The amplitude of incident and the reflected wave are showed in Fig. 6. The amplitudes are normalized by its maximum value and gathered the data from the 45 mm away from the source.

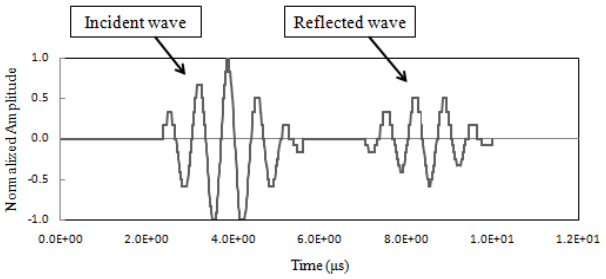


**Fig. 6** Measurement of the incident and reflected out-of-plane amplitudes (normalized), 45 mm away from the defect

To observe the energy flow in a $[0/90]_{2S}$ laminate, a flawless specimen with the operating condition is prepared and a signal of the same frequency (30 kHz) is allowed to propagate from the center of the plate. A polar diagram has been developed by gathering the out-of-plane displacement at 45 mm away from the source after excitation and illustrated in Fig. 7. The diagram indicates that the energy flow follows the stacking sequence of the laminate and influenced by the outer layer.

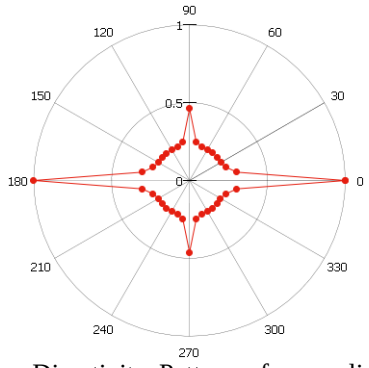


**Fig. 7** Polar Directivity Pattern of normalized out-of-plane displacement for $[0/90]_{2S}$ laminate.

For different stacking sequence of the composites, the reflected and transmitted properties of $A_0$-mode Lamb wave will be discussed in the next section.

## 4. Directivity Pattern of Scattered Wave

This section is employed for quantitative investigation of the reflected out-of-plane displacement from the defected region for CFRP laminate using the Directivity Pattern (DP) analysis. The baseline subtraction technique has been used to determine the additional out-of-plane displacement due to the reflection of the incident wave. This is achieved by conducting two simulations (each for the defected and intact laminate) with identical meshing. The out-of-plane displacement of the scattered wave $u_z^S(x,y,t)$ is determined by

$$u_z^S(x,y,t) = u_z^T(x,y,t) - u_z^I(x,y,t) \qquad (3)$$

where $u_z^T(x,y,t)$ and $u_z^I(x,y,t)$ are the space $(x,y)$ and time $(t)$ dependent out-of-plane displacement components of the defected and intact laminates, respectively. The shape is generated by calculating the absolute normalized value taken from the experiment (normalized by maximum absolute amplitude of the incident wave at the defect centre location of the intact laminate). To construct the scattering directivity pattern of the out-of-plane displacement, 24 locations with a 15º step increment have been chosen and the points are located at a distance of 45 mm away from the defect. The data has been taken at and for intact and defected laminate. Determined directivity patterns for various combination of lamina are depicted in Fig. 8.

The investigation from the calculated DP depicted a definite variation in out-of-plane amplitude almost in all radial locations. It is noteworthy that, the scattering pattern for 0º fiber direction (HTI material) is not symmetric for the symmetric cylindrical through-hole whereas for the isotropic material the scattering pattern is perfectly symmetric [6]. This significant characteristic suggests that the DP of CFRP laminate is complicated than that in the isotropic material. For the quasi-isotropic material, the DP showed in Fig. 8(e), it can be said that the scattering wave front follow the fiber direction of the outer lamina. That is the point of interest where this unique characteristic can be applied to develop a damage detecting technique focusing on the monitoring of the structural health. Furthermore, Fig. 8 suggests that the scattering out-of-plane displacement for the combination of [+45/-45] ply is smaller than the combination of [0/90] ply combination. The out-of-plane amplitudes are significantly depends on the fiber orientation of the lamina. The complexity of scattering directivity pattern increases with the numbers of lamina with different fiber direction. Such characteristic provides a significant insight into the reflecting characteristics of the low-frequency $A_0$-mode Lamb wave at through-thickness defect in CFRP laminate.

## 5. Conclusion

This paper investigated the effect of lay-up order on reflected and transmitted characteristics of the $A_0$-mode Lamb wave at a cylindrical hole in CFRP laminates. The details of 3D FE modeling and analysis on the prediction of Lamb wave propagation as well as scattering behavior have been demonstrated concisely. The dispersion characteristics, as well as the directional dependency found by the numerical study, showed quite decent agreement with that from the analytical. Composite laminates with various stacking sequences i.e. $[0/90]_{2S}$, $[0/90]_4$, $[+45/-45]_{2S}$, $[+45/-45]_4$, and $[0/+45/-45/90]_S$ have been investigated where the shape and size of the defect remained identical.

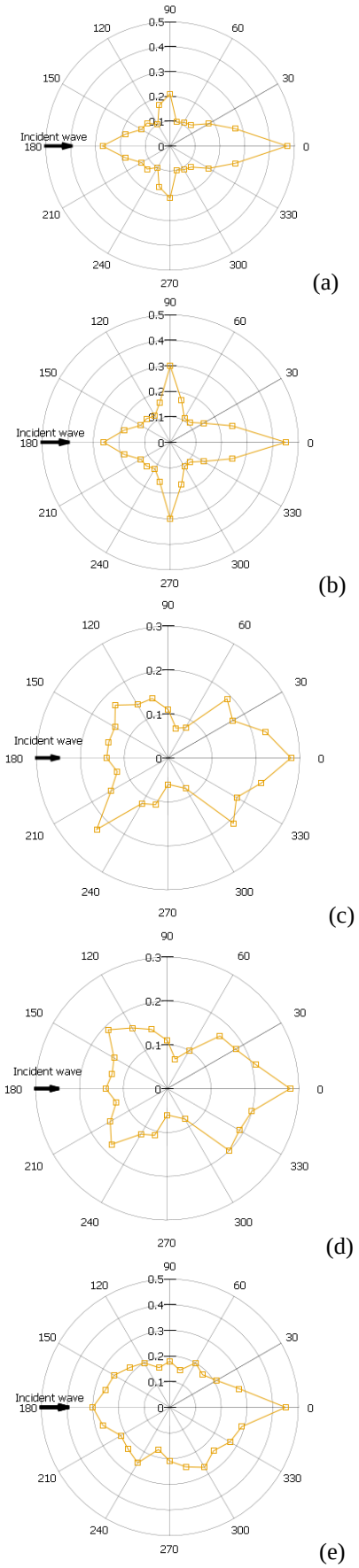


**Fig. 8** Directivity pattern of the (a) $[0/90]_{2S}$, (b) $[0/90]_4$, (c) $[+45/-45]_{2S}$, (d) $[+45/-45]_4$, (e) $[0/+45/-45/90]_S$ composite laminates.

The results depicted that, the amplitude and directivity distribution significantly influenced by the stacking sequence and influenced by the outer layer of the corresponding laminate. The outcome of this numerical study provides the idea of the effect of the stacking pattern on the reflecting characteristics of $A_0$-mode Lamb wave, leads to further development in damage detection technique for CFRP laminate.

## 6. References


[1] Guo, N., Cawley, P., The interaction of Lamb waves with delaminations in composite laminates. *The Journal of the Acoustical Society of America*, vol. 94, pp. 2240-2246, 1993.

[2] Rose, J. L., A baseline and vision of ultrasonic guided wave inspection potential. *J. Pressure Vessel Technol.*, vol. 124, pp. 273-282, 2002.

[3] Lowe, M. J., Cawley, P., Kao, J. Y., Diligent, O., The low frequency reflection characteristics of the fundamental antisymmetric Lamb wave a0 from a rectangular notch in a plate. *The Journal of the Acoustical Society of America*, vol. 112, pp. 2612-2622, 2002.

[4] Cegla, F. B., Rohde, A., Veidt, M., Analytical prediction and experimental measurement for mode conversion and scattering of plate waves at non-symmetric circular blind holes in isotropic plates, *Wave Motion*, vol. 45, pp. 162-177, 2008.

[5] Moreau, L., Castaings, M., The use of an orthogonality relation for reducing the size of finite element models for 3D guided waves scattering problems, *Ultrasonics*, vol. 48, pp. 357-366, 2008.

[6] Hayashi, T., Kawashima, K., Multiple reflections of Lamb waves at a delamination, *Ultrasonics*, vol. 40, pp. 193-197, 2002.

[7] Veidt, M., Ng, C. T., Influence of stacking sequence on scattering characteristics of the fundamental anti-symmetric Lamb wave at through holes in composite laminates, *The Journal of the Acoustical Society of America*, vol. *129*, pp. 1280-1287, 2011.

[8] Hai-Yan, Z., Jian, X., Shi-Wei, M., High-Frequency Guided Wave Scattering by a Partly Through-Thickness Hole Based on 3D Theory, *Chinese Physics Letters*, vol. *32*, 084301, 2015.

[9] Soleimanpour, R., Ng, CT., Mode conversion and scattering analysis of guided waves at delaminations in laminated composite beams, *Structural Monitoring and Maintenance*, vol. *2*: pp. 213-236, 2015.

[10] Singh, R. K., Ramadas, C., Shetty, P. B., Satyanarayana, K. G., Identification of delamination interface in composite laminates using scattering characteristics of lamb wave: numerical and experimental studies, *Smart Materials and Structures*, vol. *26*, 045017, 2017.

[11] Chiu, W. K., Rose, L. R. F., Nadarajah, N., Scattering of the fundamental anti-symmetric

Lamb wave by a mid-plane edge delamination in a fiber-composite laminate, *Procedia Engineering*, vol. *188*, pp. 317-324, 2017.
[12] Feng, B., Ribeiro, A. L., Ramos, H. G., Interaction of Lamb waves with the edges of a delamination in CFRP composites and a reference-free localization method for delamination, *Measurement*, vol. *122*, pp. 424-431, 2018.
[13] Diamanti, K., Soutis, C., Hodgkinson, J. M., Piezoelectric transducer arrangement for the inspection of large composite structures, *Composites Part A: Applied science and manufacturing*, vol. 38, pp. 1121-1130, 2007.
[14] Belanger, P., Cawley, P., Feasibility of low frequency straight-ray guided wave tomography, *NDT & E International*, vol. 42, pp. 113-119, 2009..
[15] Ng, C. T., Veidt, M., A Lamb-wave-based technique for damage detection in composite laminates, *Smart materials and structures*, vol. 18, 074006, 2009.
[16] Chamis, C. C., Mechanics of composite materials: past, present, and future, *Journal of Composites, Technology and Research*, vol. 11, pp. 3-14, 1989.
[17] Bao, M., *Analysis and design principles of MEMS devices*, Elsevier, 2005.
[18] Manual LD, Volume I. Version 971, Livermore Software Technology Corporation, 7374:354, 2007.
[19] Wu, C., Gao, Y., Fang, J., Lund, E., and Li, Q., Simultaneous discrete topology optimization of ply orientation and thickness for carbon fiber reinforced plastic-laminated structures, *Journal of Mechanical Design*, vol. *141*, 2019.
[20] Alleyne, D. N., Cawley, P., The interaction of Lamb waves with defects, *IEEE transactions on ultrasonics, ferroelectrics, and frequency control*, vol. 39, pp. 381-397, 1992.
[21] Courant, R., Friedrichs, K., Lewy, H., On the partial difference equations of mathematical physics, *IBM journal of Research and Development*, vol. 11, pp. 215-234, 1967
[22] Rose, J. L., *Ultrasonic guided waves in solid media*. Cambridge university press, 2014.